 CMES, vol.96, no.2, pp.91-101, 2013

Vortex Patches

G.R. Baker[1]

Abstract: A vortex patch is a bounded region of uniform vorticity in two-dimensional, incompressible, inviscid fluid flow. The streamfunction satisfies the Poisson equation with the vorticity acting as a source term. The standard formulation is to write the streamfunction as a convolution of the vorticity with the two-dimensional free-space Greens function. A simple application of Greens theorem converts the area integral to a boundary integral. Numerical methods must then account for the singular nature of the boundary integral, and high accuracy is difficult when filamentation takes place, that is, when long, very thin filaments of vorticity erupt from the main boundary. A new boundary integral is derived based on a different viewpoint. A particular solution is readily known which represents solid body rotation. To the particular solution must be added a homogeneous solution, and the combination must satisfy the boundary conditions. A standard boundary integral can be used to solve the Laplace equation with Dirichlet boundary conditions. This approach leads to a boundary integral without singularity and easily approximated by the trapezoidal rule that ensures spectral accuracy. Results indicate that high accuracy is possible with even modest resolution. The method is used to explore the mathematical properties of filamentation.

Keywords: Vortex Flows, Contour Dynamics, Filamentation.

1 Introduction

Given the challenges in numerically simulating fluid flow at high Reynolds numbers, researchers often turn to idealized models that contain simple distributions of vorticity under the assumption that viscosity may be neglected. In two-dimensional flow, the simplest distribution of vorticity is a vortex patch. It is a uniform distribution of vorticity bounded by a closed curve. The motion of the patch is determined completely by the motion of its boundary and an evolution equation for the boundary can be derived as a boundary integral with reference only to the location of the boundary. This approach is referred to as contour dynamics, see Pullin (1992) for

[1] The Ohio State University, Columbus, OH, USA.

a review of the early work. More recently, there has been much effort placed in extending the method to more complex flows, for example, in the presence of solid boundaries as considered by Crowdy and Surana (2007).

Perhaps the biggest success of the method of contour dynamics is the revelation of the phenomenon of filamentation by Deem and Zabusky (1978) and Dritschel (1988) whereby thin streams of vorticity are shed from the boundary of the vortex patch. The apparent consequence is that the vortex patch transforms into an essentially circular patch with uniform rotation as any perturbations are shed off as filaments. There is a companion phenomenon whereby a thin vortex layer (the infinite open vortex patch) rolls up into a central almost circular core; the thin layer takes the appearance of thin filaments that are attached to the core, see Baker and Shelley (1990).

What is clear in numerical simulations of vortex patches and vortex layers is that the curvature at the points of contact of the filaments and the main core becomes extremely high. While the boundary cannot become singular, a result first established by Chemin (1991), the high curvature introduces very small length scales and these small scales can dominate the energy spectrum. Thus it is worthwhile to examine the formation of very high curvature and to understand when it occurs. There is a natural mathematical perspective developed by Cowley, Baker, and Tanveer (1999) during studies of the formation of curvature singularities in vortex sheets, the limit of an infinitely thin vortex layer. By representing the boundary of the layer in parametric form $\big(x(p,t), y(p,t)\big)$, it is possible to find branch-point singularities in the complex p-plane that move towards the real axis and reach it in finite time, at which moment the singularities becomes physically relevant. The question arises naturally whether there are such singularities in the complex spatial plane for the location of the boundary of a vortex patch.

From experience gained by Cowley, Baker, and Tanveer (1999) in studying such singularities in vortex sheets and by Baker and Xie (2011) and Baker, Caflisch, and Siegel (1993) in other free surface flow problems, we know that highly accurate calculations of the motion of the boundary are needed to detect the presence of singularities in the complex spatial plane. Indeed, spectrally accurate methods are necessary and that in turn requires a suitable formulation of the evolution equations for the boundary. The standard formulation used in contour dynamics is not completely suitable and an alternate approach, capable of further generalizations, is presented here.

2 Evolution equations for contour dynamics

Let (x,y) be the coordinates describing a plane of two-dimensional motion. Assume the vorticity points out of the plane with uniform strength ω and is contained within a boundary given in parametric form by $\big(x(p,t),y(p,t)\big)$. The motion of the vorticity is governed by the vorticity/streamfunction formulation:

$$\frac{\partial \omega}{\partial t}+u\frac{\partial \omega}{\partial x}+v\frac{\partial \omega}{\partial y}=0\,, \tag{1}$$

where the velocity is (u,v) and the vorticity is

$$\omega=\frac{\partial v}{\partial x}-\frac{\partial u}{\partial y}\,. \tag{2}$$

The flow is assumed incompressible,

$$\frac{\partial u}{\partial x}+\frac{\partial v}{\partial y}=0\,, \tag{3}$$

which allows the introduction of the streamfunction ψ

$$u=\frac{\partial \psi}{\partial y}\,, \qquad v=-\frac{\partial \psi}{\partial x} \tag{4}$$

Upon substitution of (4) into (2), one obtains the Poisson equation for ψ given ω,

$$\nabla^2\psi=-\omega\,. \tag{5}$$

The solution to (5) must satisfy the kinematic constraints that the velocity is continuous at the boundary. The appropriate solution to (1) is found by requiring the boundary to move with the velocity at the boundary, the standard definition of Lagrangian motion.

$$\frac{\partial x}{\partial t}(p,t)=u\big(x(p,t),y)p,t)\big)\,, \qquad \frac{\partial y}{\partial t}(p,t)=v\big(x(p,t),y(p,t)\big)\,. \tag{6}$$

The standard derivation of contour dynamics introduced by N. J. Zabusky and Roberts (1979) starts with the solution to (5)

$$\psi(x,y)=-\omega\iint_A G(x-\xi,y-\eta)\,\mathrm{d}\xi\,\mathrm{d}\eta\,, \tag{7}$$

where $G(x,y)$ is the free space Greens function for the Laplacian and the integration is over the area A of the vortex patch. Consequently the velocity is given by

$$u(x,y)=-\omega\iint_A \frac{\partial G}{\partial y}(x-\xi,y-\eta)\,\mathrm{d}\xi\,\mathrm{d}\eta\,,$$

$$v(x,y)=\omega\iint_A \frac{\partial G}{\partial x}(x-\xi,y-\eta)\,\mathrm{d}\xi\,\mathrm{d}\eta\,. \tag{8}$$

Since

$$\frac{\partial G}{\partial y}(x-\xi, y-\eta) = -\frac{\partial G}{\partial \eta}(x-\xi, y-\eta),$$
$$\frac{\partial G}{\partial x}(x-\xi, y-\eta) = -\frac{\partial G}{\partial \xi}(x-\xi, y-\eta), \tag{9}$$

the integrals in (8) may be written as

$$\big(u(x,y), v(x,y)\big) = -\omega \iint_A (0,0,1) \times \nabla G(x-\xi, y-\eta)\, \mathrm{d}\xi\, \mathrm{d}\eta\,. \tag{10}$$

The integration can be reduced to integration around the boundary, and evaluating the result on the boundary produces

$$\big(u(p,t), v(p,t)\big) = -\omega \int G\big(x(p,t)-x(q,t), y(p,t)-y(q,t)\big)\,\big(x_q(q), y_q(q)\big)\,\mathrm{d}q\,. \tag{11}$$

The subscripts q refer to differentiation. Once the integral (11) has been performed, the results may be used in (6) to advance the location of the boundary. The particularly pleasing aspect of the result is that the evolution of the boundary depends only on the location of the boundary and thus represents a reduction in spatial dimension.

Since G contains the natural logarithm, the integral is weakly singular and is not conducive to highly accurate numerical integration. An alternate approach is to pick a particular solution for (5) valid inside the patch and add a homogeneous solution. The obvious choice is

$$\psi_i = -\frac{\omega}{4} r^2 + \tilde{\psi}_i \tag{12}$$

inside the patch, while

$$\psi_o = -\frac{\omega R^2}{2} \ln r + \tilde{\psi}_o \tag{13}$$

outside the patch. The area of the patch is written as $A = \pi R^2$. Both $\tilde{\psi}_i$ and $\tilde{\psi}_o$ must satisfy Laplace's equation and the solutions are connected by the requirement that ψ and its normal derivative are continuous at the boundary.

The continuity of ψ requires

$$\tilde{\psi}_o(p) - \tilde{\psi}_i(p) = \omega \left[\frac{R^2}{2} \ln\big(r(p)\big) - \frac{1}{4} r^2(p)\right] \tag{14}$$

where $r^2(p) = x^2(p) + y^2(p)$. The continuity of the normal derivative of ψ requires

$$s_p(p)\left(\frac{\partial\tilde{\psi}_o}{\partial n}(p) - \frac{\partial\tilde{\psi}_i}{\partial n}(p)\right) = \frac{\omega}{2}\,\frac{x(p)\,y_p(p) - y(p)\,x_p(p)}{r^2(p)}\left(R^2 - r^2(p)\right) \tag{15}$$

where the subscripts p refer to differentiation and $s_p^2(p) = x_p^2(p) + y_p^2(p)$.

Represent $\tilde{\psi}$ by a dipole distribution $\mu(p)$ and a source distribution $\sigma(p)$ along the boundary.

$$\tilde{\psi} = \Re\left\{\frac{1}{2\pi\mathrm{i}}\int\frac{\mu(q)}{z - z(q)}\,z_q(q)\,\mathrm{d}q + \frac{1}{2\pi}\int\sigma(q)\,\ln|z - z(q)|\,s_q(q)\,\mathrm{d}q\right\} \tag{16}$$

where $z = x + \mathrm{i}y$ is a location in complex form and $z(p) = x(p) + \mathrm{i}y(p)$ marks the location of the boundary: $z_p(p) = x_p(p) + \mathrm{i}y_p(p)$. The complex form of the boundary integrals proves useful for two-dimensional free surface flow in general as noted by Baker (2010). This representation has the important following properties: the dipole strength is given by

$$\mu(p) = \tilde{\psi}_o(p) - \tilde{\psi}_i(p) \tag{17}$$

and accounts for the jump in the stream function in (14), and the source strength is given by

$$\sigma(p) = \frac{\partial\tilde{\psi}_o}{\partial n}(p) - \frac{\partial\tilde{\psi}_i}{\partial n}(p)\,. \tag{18}$$

The combination is successful because the contribution from the dipole strength has a continuous normal derivative while the contribution from the source distribution is continuous across the boundary.

There is a further advantage to (16). The harmonic conjugate to $\tilde{\psi}$ is $-\tilde{\phi}$ so that $\tilde{\Psi} = \tilde{\psi} - \mathrm{i}\tilde{\phi}$ is analytic and is given by

$$\tilde{\Psi} = \frac{1}{2\pi\mathrm{i}}\int\frac{\mu(q)}{z - z(q)}\,z_q(q)\,\mathrm{d}q + \frac{1}{2\pi}\int\nu(q)\,\ln(z - z(q))\,\mathrm{d}q\,, \tag{19}$$

where $\nu(p) = \sigma(p)s_p(p)$.

We are now in a position to calculate the velocity at the boundary. Let $w = u + \mathrm{i}v$ be the complex form of the velocity with components (u, v). then

$$w^* = \mathrm{i}\frac{\mathrm{d}\Psi}{\mathrm{d}z} \tag{20}$$

where the star superscript indicates complex conjugation. While the stream function has been decomposed into two parts in each region, the velocity is unique at the boundary and can be calculated by taking the average value of the two representations there. Thus

$$w^*(p) = -\mathrm{i}\frac{\omega}{4}z^*(p) - \mathrm{i}\frac{\omega R^2}{4}\frac{1}{z(p)} + \frac{\mathrm{i}}{z_p(p)}\frac{\mathrm{d}\tilde{\Psi}}{\mathrm{d}p}(p) \tag{21}$$

where the derivative of $\tilde{\Psi}(p)$ contains the principle value of the integrals that arise from (19). This derivative may be rewritten as

$$\begin{aligned}\frac{1}{z_p(p)}\frac{\mathrm{d}\tilde{\Psi}}{\mathrm{d}p}(p) &= -\frac{1}{2\pi\mathrm{i}}\int\frac{\mu(q)\,z_q(q)}{\big(z(p)-z(q)\big)^2}\,\mathrm{d}q + \frac{1}{2\pi}\int\frac{\nu(q)}{z(p)-z(q)}\,\mathrm{d}q\\ &= \frac{1}{2\pi\mathrm{i}}\int\frac{\mu_q(q)+\mathrm{i}\nu(q)}{z(p)-z(q)}\,\mathrm{d}q\,,\end{aligned} \tag{22}$$

where integration by parts has been used on the first integral.

From (14) and (15),

$$\mu_p(p) + \mathrm{i}\nu(p) = \frac{\omega z_p(p)}{2}\left(\frac{R^2}{z(p)} - z^*(p)\right) \tag{23}$$

By the calculus of residues, the principle value of the integral

$$\frac{1}{2\pi\mathrm{i}}\int\frac{1}{z(p)-z(q)}\,\frac{z_q(q)}{z(q)}\,\mathrm{d}q = \frac{1}{2z(p)}\,. \tag{24}$$

So the velocity becomes

$$w^*(p) = -\mathrm{i}\,\frac{\omega}{4}\,z^*(p) - \frac{\omega}{4\pi}\int\frac{z^*(q)\,z_q(q)}{z(p)-z(q)}\,\mathrm{d}q\,, \tag{25}$$

which may be rewritten in a more convenient form

$$w^*(p) = \frac{\omega}{4\pi}\int\frac{z^*(p)-z^*(q)}{z(p)-z(q)}\,z_q(q)\,\mathrm{d}q\,. \tag{26}$$

This form is the same as that derived by Pullin (1981) by integration by parts of (11).

The main advantage in the derivation presented here is that this approach can be easily combined with methods to track free surface between fluids of different densities and moving solid boundaries as described by Baker (2010).

3 Numerical method and results

Because the boundary of the vortex patch is closed, the integrand is periodic. The trapezoidal rule provides a spectrally accurate approximation but to apply it to (26), the limiting form of the integrand must be calculated as $q \to p$. A simple calculation provides the limit $z_p^*(p)$. On the other hand, it is easy to rewrite (26) in a form where the limit proves to be zero:

$$\frac{\partial z^*}{\partial t}(p) = \frac{\omega}{4\pi} \int \left(\frac{z_q(q)}{z(p) - z(q)} - \frac{z_q^*(q)}{z^*(p) - z^*(q)} \right) \left(z^*(p) - z^*(q) \right) \mathrm{d}q \tag{27}$$

The boundary is partitioned into N points z_j equally spaced in p and the derivatives $z_{p,j}$ are obtained by analytic differentiation of the truncated Fourier series representation of $z(p)$. The Fourier coefficients are obtained through the use of the Fast Fourier Transform. The trapezoidal rule is applied to (27). Thus the following system of ordinary differential equations in time is obtained.

$$\frac{\mathrm{d}z_j^*}{\mathrm{d}t} = \frac{\omega}{2N} \sum_{k=0}^{N-1} \left(\frac{z_{q,k}}{z_j - z_k} - \frac{z_{q,k}^*}{z_j^* - z_k^*} \right) \left(z_j^* - z_k^* \right) \tag{28}$$

The initial condition

$$z(p) = \mathrm{e}^{\mathrm{i}p} + \delta\, \mathrm{e}^{2\mathrm{i}p} \tag{29}$$

is chosen because it leads to the formation of a single filament and makes the study of the behavior of the curvature simpler. It also provides a challenging test case of the method. The choice $\omega = 1$ and $\delta = 0.35$ is made and the evolution of the boundary of the patch is shown in Fig. 1 as a series of snapshots at times $t = 0, \pi, 2\pi, 3\pi$. A time step of $\triangle t = \pi/160$ is used with $N = 2048$ surface markers.

Clearly visible is the formation of a filament. Two regions of high curvature are evident, one at the tip of the filament and the other where the filament joins the main part of the patch. The profile of the curvature

$$\kappa(p) = \frac{x_p(p) y_{pp} - y_p(p) x_{pp}}{\left(x_p^2(p) + y_p^2(p) \right)^{3/2}}, \tag{30}$$

is shown in Fig. 2 at $t = 3\pi$. The very sharp spike is the curvature at the tip of the filament, while the shallower dip in curvature occurs near the attachment point. The profile of the curvature is well resolved by the number of markers used.

An interesting perspective on the behavior of the curvature comes from previous studies of singularity or near singularity formation in free surface flows, for example, by Baker and Xie (2011). They consider the analytic continuation of the

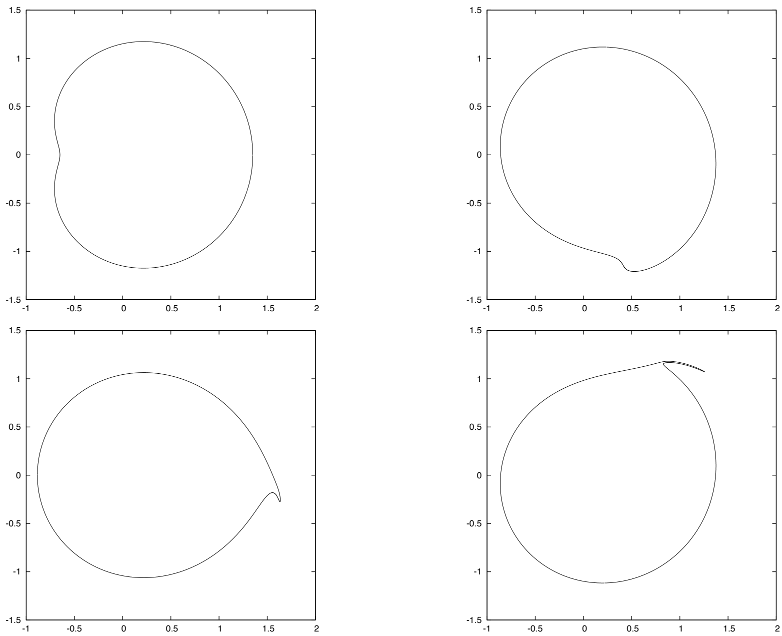

Figure 1: Time sequences of the vortex patch boundary from left to right, top to bottom: the times are $t = 0, \pi, 2\pi, 3\pi$.

curvature into the complex p-plane.

$$\kappa(p) = \frac{-\mathrm{i}}{2\sqrt{z_p^* z_p}} \left(\frac{z_{pp}}{z_p} - \frac{z_{pp}^*}{z_p^*} \right). \tag{31}$$

Singularities in the curvature may arise from singularities in the complex plane for $z(p)$ or from zeros in $z_p(p)$, and both have been found in several different studies of free surface flows. For vortex sheets, the singularities are 3/2-power branch points; see Cowley, Baker, and Tanveer (1999). These branch point singularities are also present in studies of the two-fluid Rayleigh-Taylor instability; see Baker, Caflisch, and Siegel (1993). For classical water waves, where the air is treated essentially as a vacuum, the singularities in the curvature result from zeros in $z_p(p)$, in particular, they occur very near to the tip of a plunging breaker; see Baker and Xie (2011). For periodic vortex layers, the singularities are of 3/2-power branch point type, but it is worth noting that the filaments that form in time join smoothly with the vortex cores. In other words, the filaments do not have tips; see Baker and Shelley (1990). In all these studies, both theory and numerical simulations support the presence of 3/2-power branch point singularities and zeros of $z_p(p)$ that move about the

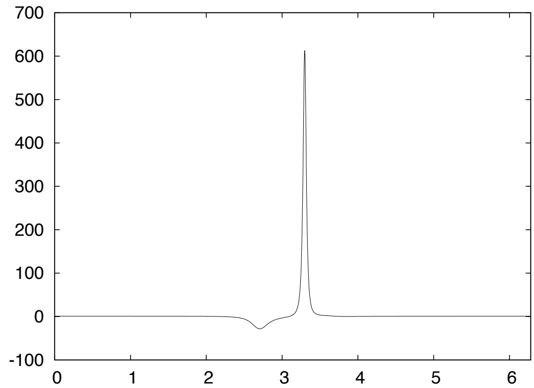

Figure 2: The curvature of the vortex patch boundary at $t = 3\pi$.

complex p-plane while retaining their form. In some cases they reach the real axis in finite time, when the singularity has physical relevance. In other cases, they approach the real axis very closely, inducing places of high curvature. It is this case that is of relevance for vortex patches.

Singularities in the complex plane can be detected through the behavior of the Fourier series as described by Sulem, Sulem, and Frisch (1983). This method was applied to detect the presence of a 3/2-power branch point. On the other hand, zeros in $z_p(p)$ can be detected and traced by simply using Newton's method on the analytic continuation of the Fourier series. This works as long as the zeros are within the strip of analyticity of the Fourier series, which is limited by the presence of the 3/2-power branch points. The location of the zeros in $z_(p)$ and the 3/2-power branch point are shown in Fig. 3. The location of the branch point is shown for only two times, but it can be traced for later times; it is marked with $\triangle$. The intent is to show its location up to $t = 2\pi$ for comparison with the location of the dominant zero in $z_p(p)$. One of the zeros in $z_p(p)$, marked with $\Box$, is present initially and approaches the real axis, but is overtaken by both the 3/2-power branch point and the other zero. Its location is shown up to $t = 3\pi/2$ and no further because the 3/2-power branch point has moved closer to the real axis and limits the strip of analyticity of the Fourier series; the location of the zero can no long be determined by the analytic continuation of the Fourier series. The dominant zero appears to move in very quickly from infinity. It is marked with $\bigcirc$. It approaches the real axis very closely and is the cause of the very high curvature at the tip of the filament, while the 3/2-power branch point is associated with the high curvature that forms where the filament attaches to the vortex core.

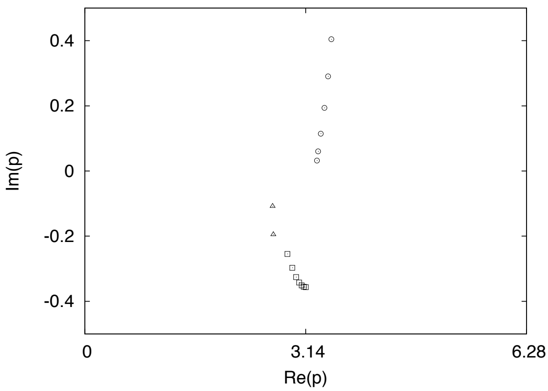

Figure 3: The location of a 3/2-power branch point (△) at $t = 7\pi/4, 2\pi$. Also shown are the location of two zeros in $z_p(p)$: one (□) is shown at $t = 0, \pi/4, \pi/2, 3\pi/4, \pi, 5\pi/4, 3\pi/2$ and the other (○) is shown at $t = \pi/2, 3\pi/4, \pi, 5\pi/4, 3\pi/2, 7\pi/4, 2\pi$.

4 Conclusions

By restating the evolution equations for the boundary of a vortex patch, a spectrally accurate method has been developed that allows highly accurate Fourier spectra to be computed. These spectra are needed to detect singularities in the complex plane of the parametrization variable for the boundary of the patch. Results indicate the formation of a very thin filament that sheds from the vortex core with a very sharp tip. The presence of a 3/2-power branch point is detected that approaches the real axis where the filament attaches to the core, while a zero in $z_p(p)$ also approaches the real axis very closely and is associated with the very sharp tip. It appears likely that this behavior is typically in free surface flows that form regions of high curvature.

Acknowledgement: I am deeply indebted to Giorgio Riccardi, Dept. of Aerospace and Mechanical Engineering, II University of Naples, Italy, for many stimulating discussions and correspondence.

References

Baker, G. R. (2010): *Boundary Element Methods in Engineering and Sciences*. Imperial College Press.

Baker, G. R.; Caflisch, R. E.; Siegel, M. (1993): Singularity formation during Rayleigh-Taylor instability. *J. Fluid Mech.*, vol. 252, pp. 51–78.

Baker, G. R.; Shelley, M. J. (1990): On the connection between thin vortex layers and vortex sheets. *J. Fluid Mech.*, vol. 15, pp. 161–194.

Baker, G. R.; Xie, C. (2011): Singularities in the complex physical plane for deep water waves. *J. Fluid Mech.*, vol. 685, pp. 83–116.

Chemin, J. Y. (1991): Existence globalle pour le problème des poches de tourbillon. *CR Acad. Sci. Paris Ser. I.*, vol. 312, pp. 803–806.

Cowley, S. J.; Baker, G. R.; Tanveer, S. (1999): On the formation of Moore curvature singularities in vortex sheets. *J. Fluid Mech.*, vol. 378, pp. 233–267.

Crowdy, D.; Surana, A. (2007): Contour dynamics in complex domains. *J. Fluid Mech.*, vol. 593, pp. 235–254.

Deem, G. S.; Zabusky, N. J. (1978): Vortex waves: stationary 'V' states, interactions, recurrence and breaking. *Phys. Rev. Lett.*, vol. 40, pp. 859–862.

Dritschel, D. G. (1988): The repeated filamentation of two-dimensional vorticity interfaces. *J. Fluid Mech.*, vol. 194, pp. 511–547.

N. J. Zabusky, M. H. H.; Roberts, K. V. (1979): Contour dynamics for the Euler equation in two dimensions. *J. Comput. Phys.*, vol. 30, pp. 96–106.

Pullin, D. I. (1981): The nonlinear behavior of a constant vorticity layer at a wall. *J. Fluid Mech.*, vol. 108, pp. 401–421.

Pullin, D. I. (1992): Contour dynamics methods. *Ann. Rev. Fluid Mech.*, vol. 24, pp. 89–115.

Sulem, C.; Sulem, P.-L.; Frisch, H. (1983): Tracing complex singularities with spectral methods. *J. Comput. Phys.*, vol. 50, pp. 138–161.